Molecular Therapy
Nucleic Acids
Original Article

# circ-NOL10 regulated by MTDH/CASC3 inhibits breast cancer progression and metastasis via multiple miRNAs and PDCD4

Yujie Cai,[1,2,6] Xing Zhao,[1,3,6] Danze Chen,[1] Fan Zhang,[1] Qiuyang Chen,[1] Chang-Chun Shao,[4] Yan-Xiu Ouyang,[4] Jun Feng,[5] Lili Cui,[2] Min Chen,[5] and Jianzhen Xu[1]

[1]Systems Biology Lab, Shantou University Medical College (SUMC), 515041 Shantou, China; [2]Guangdong Key Laboratory of Age-Related Cardiac and Cerebral Diseases, Affiliated Hospital of Guangdong Medical University, 524000 Zhanjiang, China; [3]Department of Pathology and Medical Biology, University of Groningen, University Medical Center, Groningen, 9700 RB Groningen, the Netherlands; [4]ChangJiang Scholar's Laboratory, Shantou University Medical College (SUMC), 515041 Shantou, China; [5]Clinical Central Research Core, Xiang'an Hospital of Xiamen University, No. 2000, Xiang'an Road East, Xiamen, 361101 Fujian, China

**Circular RNAs (circRNAs) play important roles in carcinogenesis. Here, we investigated the mechanisms and clinical significance of *circ-NOL10*, a highly repressed circRNA in breast cancer. Subsequently, we also identified RNA-binding proteins (RBPs) that regulate *circ-NOL10*. Bioinformatics analysis was utilized to predict regulatory RBPs as well as *circ-NOL10* downstream microRNAs (miRNAs) and mRNA targets. RNA immunoprecipitation, luciferase assay, fluorescence *in situ* hybridization, cell proliferation, wound healing, Matrigel invasion, cell apoptosis assays, and a xenograft model were used to investigate the function and mechanisms of *circ-NOL10* *in vitro* and *in vivo*. The clinical value of *circ-NOL10* was evaluated in a large cohort of breast cancer by quantitative real-time PCR. *Circ-NOL10* is downregulated in breast cancer and associated with aggressive characteristics and shorter survival time. Upregulation of *circ-NOL10* promotes apoptosis, decreases proliferation, and inhibits invasion and migration. Furthermore, *circ-NOL10* binds multiple miRNAs to alleviate carcinogenesis by regulating PDCD4. CASC3 and metadherin (MTDH) can bind directly to *circ-NOL10* with characterized motifs. Accordingly, ectopic expression or depletion of CASC3 or MTDH leads to *circ-NOL10* expression changes, suggesting that these two RBPs modulate *circ-NOL10* in cancer cells. *circ-NOL10* is a novel biomarker for diagnosis and prognosis in breast cancer. These results highlight the importance of therapeutic targeting of the RBP-noncoding RNA (ncRNA) regulation network.**

## INTRODUCTION

Breast cancer is the most common and heterogeneous disease among women in the world.[1] Despite continuous development of early diagnosis and improvement of treatments over the past few decades, there are still limited efficient therapies, especially in subtypes such as triple-negative breast cancer (TNBC). The median overall survival is only 10–13 months for metastatic TNBC.[2] Therefore, understanding the molecular pathogenesis involved in cancer development and identifying novel biomarkers are essential to determine diagnosis, treatment strategies, and prognosis. Over the last few years, accumulating reports have found that noncoding RNAs (ncRNAs), including circular RNAs (circRNAs), are implicated widely in breast cancer progression.[3,4]

circRNA is a circular form of endogenous ncRNA produced mainly by circularization of specific exons. Expression analyses have indicated that it is tissue- or developmental stage-specific and evolutionarily conserved between mice and humans.[5,6] A variety of molecular mechanisms have been proposed to explain circRNA function in human cancer, including acting as microRNA (miRNA) decoys, regulating gene splicing or transcription, translating peptides, and epigenetic regulation.[4,7,8] Further, circRNAs are stable in formalin-fixed, paraffin-embedded tissue and human biofluids, such as exosomes, saliva, and plasma, indicating their potential diagnostic values[9–11]

In breast cancer, we and others have discovered that several circRNAs inhibit tumor progression or promote tumorigenesis.[12–14] For example, circEPSTI1 has been found to be increased significantly in TNBC samples. This circRNA is also a prognostic marker.[14] Using a high-throughput circRNA microarray profiling platform, we identified a set of significantly decreased circRNAs in a large cohort of individuals with breast cancer. We elucidated the functions and molecular mechanisms of *circTADA2As* in breast cancer. Among these differentially expressed circRNAs, *circ-NOL10* was the most downregulated in TNBC samples. In this study, we first investigated the clinical significance of *circ-NOL10*. Subsequently, we explored its biological roles and molecular mechanism during breast cancer progression. Furthermore, our bioinformatics analysis predicted that two RBPs (metadherin

Received 20 November 2020; accepted 24 September 2021;
https://doi.org/10.1016/j.omtn.2021.09.013.

[6]These authors contributed equally

**Correspondence:** Jianzhen Xu, Systems Biology Lab, Shantou University Medical College (SUMC), 515041 Shantou, China.
**E-mail:** jzxu01@stu.edu.cn
**Correspondence:** Min Chen, Clinical Central Research Core, Xiang'an Hospital of Xiamen University, No. 2000, Xiang'an Road East, Xiamen, 361101, Fujian, China
**E-mail:** mchen@xah.xmu.edu.cn

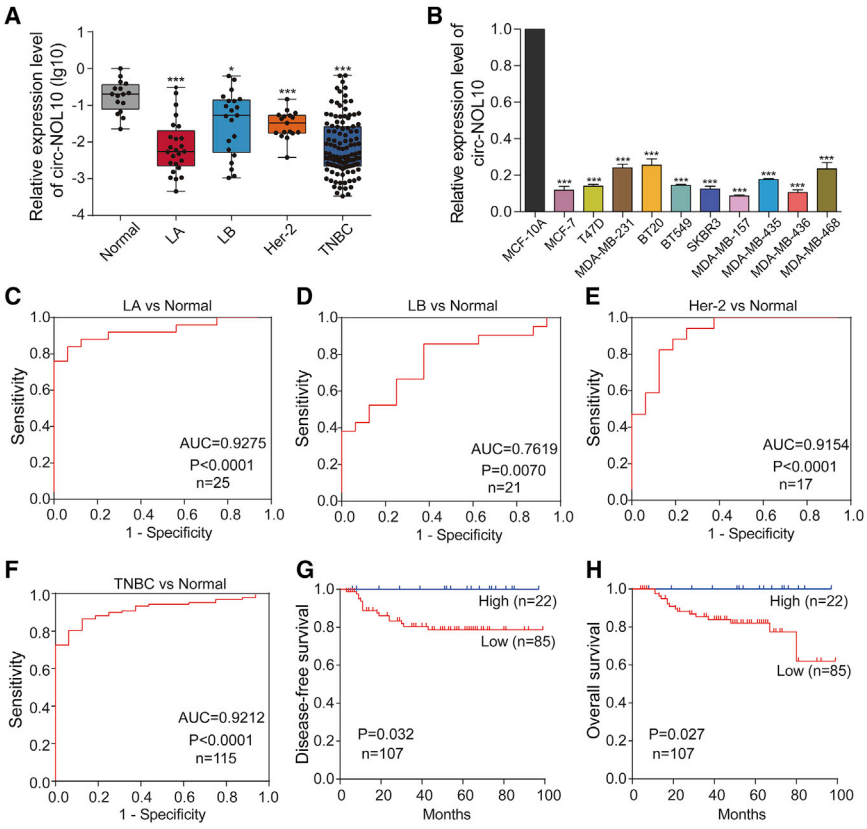


**Figure 1. Decreased expression of circ-NOL10 in breast cancer and clinical implications**

(A) circ-NOL10 was significantly lower in breast cancer tissue. Shown is relative expression of circ-NOL10 in 178 breast cancer tissues (LA, N = 25; LB, N = 21; Her-2, N = 17; TNBC, N = 115) and 16 normal mammary gland tissues; each point represents one tissue sample. (B) circ-NOL10 was significantly lower in breast cancer cells. Shown is relative expression of circ-NOL10 in 10 breast cancer cell lines compared with MCF-10A cells. (C-F) ROC curve of circ-NOL10 in LA(C), LB (D), Her-2(E) and TNBC (F) using normal mammary gland tissues as control. (G and H) Kaplan-Meier analyses of the association between circ-NOL10 and DFS (G) or OS (H) in individuals with TNBC. Error bars represent the mean ± SEM from three independent experiments. *p < 0.05, ***p < 0.001.

[MTDH] and CASC3 exon junction complex subunit [CASC3]) can directly bind to *circ-NOL10*, which is confirmed by follow-up experiments. Overall, we identified a novel RBP-ncRNA signaling route formed by two RBPs (*MTDH* and *CASC3*), one circRNA (*circ-NOL10*), three miRNAs (*miR-149-5p*, *miR-330-3p*, and *miR-452-5p*), and the effector PDCD4 in breast cancer carcinogenesis.

## RESULTS

### *Circ-NOL10* is downregulated in breast cancer and associated with aggressive characteristics

We performed qPCR analyses on 178 breast cancer tissues (LA, N = 25; LB, N = 21; Her-2, N = 17; TNBC, N = 115) and 16 normal mammary gland tissues. Expression of *circ-NOL10* is significantly lower in breast cancer tissue, which is consistent with our previous finding by circRNA array.[13] The reduction of *circ-NOL10* is more evident in LA and TNBC tissues (Figure 1A). Correspondingly, the expression levels of *circ-NOL10* in 10 breast cancer cell lines were lower than in the immortalized mammary gland cell line MCF-10A (Figure 1B).

Notably, decreased *circ-NOL10* expression is correlated significantly with advanced clinical stage (p = 0.018), increased lymphatic metastasis (p = 0.032), recurrence (p = 0.001), and death (p = 0.001) in individuals with TNBC (Table 1). These results suggest an association between downregulation of *circ-NOL10* and aggressive characteristics of TNBC. Receiver operating characteristic (ROC) curves for *circ-NOL10* were calculated. The area under the curve (AUC) for TNBC was 0.9212 (p < 0.0001; Figure 1F). Additionally, the AUCs for LA, LB, and Her-2 were 0.9275, 0.7619, and 0.9154, respectively (Figures 1C–1E), indicating that *circ-NOL10* might be a promising diagnostic indicator for breast cancer. Next, according to the cutoff value of the ROC curve, individuals with TNBC were divided into two groups for disease-free survival (DFS) and overall survival (OS) analyses. Interestingly, low *circ-NOL10* expression was significantly related to shorter DFS (p = 0.032) and OS (p = 0.027) (Figures 1G and 1H). Univariate Cox proportional hazards regression analyses indicated that *circ-NOL10*, like clinical stage, T classification status, and lymphatic metastasis, is a risk factor for DFS of individuals with TNBC (HR = 4.616, p = 0.043) and OS (HR = 3.886, p = 0.045) but not an independent prognostic factor for poor DFS and OS in the multivariate Cox model (Tables S1 and S2).

### *Circ-NOL10* inhibits breast cancer progression and metastasis

In view of *circ-NOL10* being downregulated in breast tissue and cell lines, we overexpressed *circ-NOL10* to further study its potential function in the MDA-MB-231 and MCF-7 cell lines. As shown in Figure 2A, ectopic expression of *circ-NOL10* was increased significantly, indicating good overexpression efficiency. Upregulation of *circ-NOL10* decreased cell proliferation (Figure 2B) and inhibited colony formation and invasion (Figures 2C–2D). Moreover, the wound healing assay demonstrated that ectopic expression of *circ-NOL10* significantly inhibited migration of MDA-MB-231 and MCF-7 cells (Figure 2E). In addition, we investigated whether *circ-NOL10* affects cell apoptosis using a flow cytometry assay. The results showed that early apoptosis could be triggered by *circ-NOL10* overexpression but late apoptosis could not (Figure 2F).

To further confirm the function of *circ-NOL10*, we designed two small interfering RNA (siRNA)-circ-NOL10 products

**Table 1. Correlation between clinicopathological factors and circ-NOL10 expression level in TNBC tissue (n = 115)**

| Characteristics | No. of individuals (%) | Mean ± SEM | p value |
|---|---|---|---|
| Age | | | |
| ≥55 | 42 (36.5%) | 0.02803 ± 0.00828 | 0.364 |
| < 55 | 73 (63.5%) | 0.04637 ± 0.01447 | |
| AJCC TNM stage[a] | | | |
| I–II | 82 (74.5%) | 0.04876 ± 0.01331 | 0.018* |
| III–IV | 28 (25.5%) | 0.01451 ± 0.00507 | |
| T classification[b] | | | |
| $T_{1-2}$ | 95 (91.3%) | 0.04540 ± 0.01159 | 0.296 |
| $T_{3-4}$ | 9 (8.7%) | 0.00568 ± 0.00331 | |
| Lymphatic metastasis | | | |
| $N_{0-1}$ | 91 (79.1%) | 0.04576 ± 0.01207 | 0.032* |
| $N_{2-3}$ | 24 (20.9%) | 0.01660 ± 0.00583 | |
| Relapse[c] | | | |
| No | 91 (85.0%) | 0.04837 ± 0.01207 | 0.001** |
| Yes | 16 (15.0%) | 0.00502 ± 0.00150 | |
| Survival[c] | | | |
| Yes | 92 (86.0%) | 0.04786 ± 0.011945 | 0.001** |
| No | 15 (14.0%) | 0.00525 ± 0.00160 | |

AJCC, American Joint Committee on Cancer. *p < 0.05, **p < 0.01.
[a]4.35% patient information missing.
[b]9.57% patient information missing.
[c]6.96% patient information missing.

(circ-NOL10 siRNA#1 and siRNA#2) that could efficiently knock down expression of *circ-NOL10* in cells (Figure 3A). Then alterations in proliferative capacity were evaluated using a CCK-8 assay. The results showed that depletion of *circ-NOL10* could increase proliferation of breast cancer cells (Figure 3B). Furthermore, silencing *circ-NOL10* expression significantly increased colony formation ability, migration, and invasion in MDA-MB-231 and MCF-7 cells (Figures 3C–3E). Flow cytometry results also showed that silencing *circ-NOL10* by siRNAs decreased apoptosis (Figure 3F). Similar cellular function was also observed by siRNA treatment in MCF-10A cells, which expressed higher *circ-NOL10* (Figure S1). These results suggest that *circ-NOL10* plays a vital role in cell carcinogenesis.

### *Circ-NOL10* reduces tumor growth *in vivo*

To study the function of *circ-NOL10 in vivo*, MDA-MB-231 cells were stably transfected with Lv-circ-NOL10 or Lv-circ-control and inoculated subcutaneously into nude mice. The tumors were monitored over a period of 21 days. The tumor volumes of the Lv-circ-NOL10 group were significantly smaller than those of the control group (Figures 4A–4C). A qPCR assay confirmed that *circ-NOL10* expression was higher in *circ-NOL10* overexpression mice (Figure 4D). Thus, the xenograft tumor model verified that *circ-NOL10* can inhibit BC tumor growth *in vivo*.

### *Circ-NOL10* interacts with and sequesters miR-149-5p, miR-330-3p, and miR-452-5p

To explore the molecular mechanism of *circ-NOL10* in breast cancer, we determined the subcellular location of *circ-NOL10* in MDA-MB-231 and MCF-7 cells with fluorescence *in situ* hybridization (FISH). As shown in Figure 5A, *circ-NOL10* was expressed in the cytoplasm and nucleus in cancer cells. Previous studies have demonstrated that some circRNAs can function as miRNA sponges in breast cancer,[13,15] so we combined several bioinformatics tools to predict miRNAs that potentially bind to *circ-NOL10* (Figure 4B). Furthermore, we used the mirgator.kobic3.0 database to select eight miRNAs that are expressed abundantly in breast cancer tissues and have binding sites on *circ-NOL10* (Figure 4C). Next, *miR-149-5p*, *miR-330-3p*, *miR-452-5p*, and *miR-767-5p* were selected manually for experimental verification. Dual-luciferase reporter assays were performed with a recombinant reporter plasmid containing a luciferase gene and the *circ-NOL10* sequence (psiCHECK2-circ-NOL10). A schematic of psiCHECK2-circ-NOL10 and *circ-NOL10* recognition sites is shown in Figure 5D. Co-transfected psiCHECK2-circ-NOL10 and *miR-149-5p*, *miR-330-3p*, and *miR-452-5p* significantly decreased firefly luciferase reporter activity, but there was no significant change for co-transfected psiCHECK2-NOL10 and *miR-767-5p* (Figure 5E). These results indicate that *miR-149-5p*, *miR-330-3p*, and *miR-452-5p* can bind to *circ-NOL10*. Furthermore, the relative expression of *miR-149-5p*, *miR-330-3p*, and *miR-452-5p* were reduced significantly after overexpression of *circ-NOL10* in breast cancer cells (Figure 5F). Finally, we checked cellular apoptosis after co-transfection of these miRNAs or *circ-NOL10* alone in cells. We found that overexpression of these three miRNAs in the *circ-NOL10*-treated group can significantly decrease cellular apoptosis in MDA-MB-231 and MCF-7 cells (Figures 5G and 5H). These results confirmed our hypothesis that *circ-NOL10* can interact with and sequester *miR-149-5p*, *miR-330-3p*, and *miR-452-5p* in breast cancer.

### *Circ-NOL10* suppresses carcinogenesis by regulating *PDCD4*

Next we combined five bioinformatic databases (TargetScan, miRNAorg, PITA, PicTar, and miRDB) to analyze the potential miRNA targets. Four genes (*TUSC2*, *PDCD4*, *GRIA3*, and *CCBE1*) were selected based on overlap of these prediction results for follow-up experimental verification (Figure S2A). After ectopic expression of *circ-NOL10*, we found that only *PDCD4* was increased significantly compared with vector transfection at the protein level (Figures S2B and S2C). Because miRNAs generally regulate target gene expression by inhibiting translation, we decided to focus on *PDCD4* in the following experiments. As a tumor suppressor with multi-functions, *PDCD4* has been reported to be involved in proliferation, migration, invasion, and apoptosis.[16–18] Downregulation of *PDCD4* was also associated with poor prognosis in previous studies.[19,20] Importantly, it is a known target gene for *miR-330-3p* in esophageal cancer.[21] After transfection of the *circ-NOL10* plasmid or *circ-NOL10* siRNAs, the protein level of *PDCD4* was increased accordingly in *circ-NOL10*-overexpressing cells and decreased in siRNA *circ-NOL10*-treated cells (Figure 6A). Then we used two different siRNAs to inhibit expression of *PDCD4* (Figure 6B). As shown in Figures 6C–6G, cell invasion,

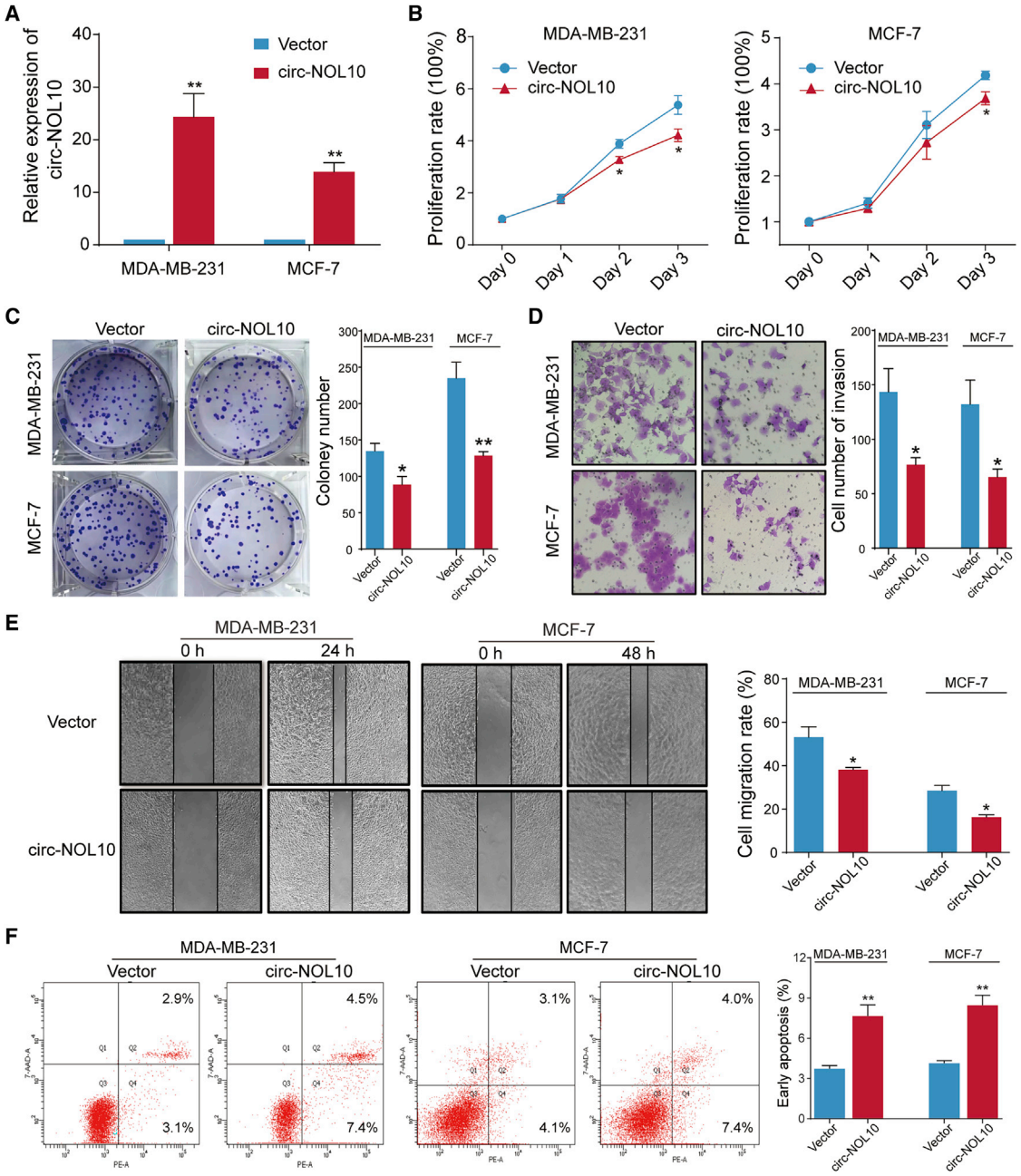


**Figure 2. circ-NOL10 suppresses cancer progression**

Experiments were conducted after transfecting MCF-7 and MDA-MB-231 cells with a circ-NOL10-expressing vector for 48 h. (A) Ectopic circ-NOL10 expression was analyzed by qPCR. (B) The effect of circ-NOL10 on cell viability was analyzed by CCK-8. (C) The effect of circ-NOL10 on colony formation was determined via a clonogenicity assay (left, representative pictures; right, quantitative bar for colony numbers). (D) The effect of circ-NOL10 on cell invasion was detected via a Transwell assay (left, morphological comparison of cell penetration; right, quantitative bar for number of penetrating cells). (E) The effect of circ-NOL10 on cell migration was measured by a wound scratch assay (left, representative images; right, quantitative bar for cell migration rate). (F) The effect of circ-NOL10 on early apoptosis was analyzed by flow cytometry in cells (left, representative images; right, quantitative bar for cell apoptosis rate). Error bars represent the mean ± SEM from three independent experiments. *$p < 0.05$, **$p < 0.01$.

migration, and apoptosis assays indicated that knockdown of *PDCD4* partially abolishes the effects of *circ-NOL10* on breast cancer cells. Additionally, western blotting was performed to examine whether *PDCD4* protein expression was affected by *miR-149-5p*, *miR-330-3p*, and *miR-452-5p*. In MDA-MB-231 cells, a fluorescence-activated cell sorting (FACS)-based assay indicated that apoptosis was

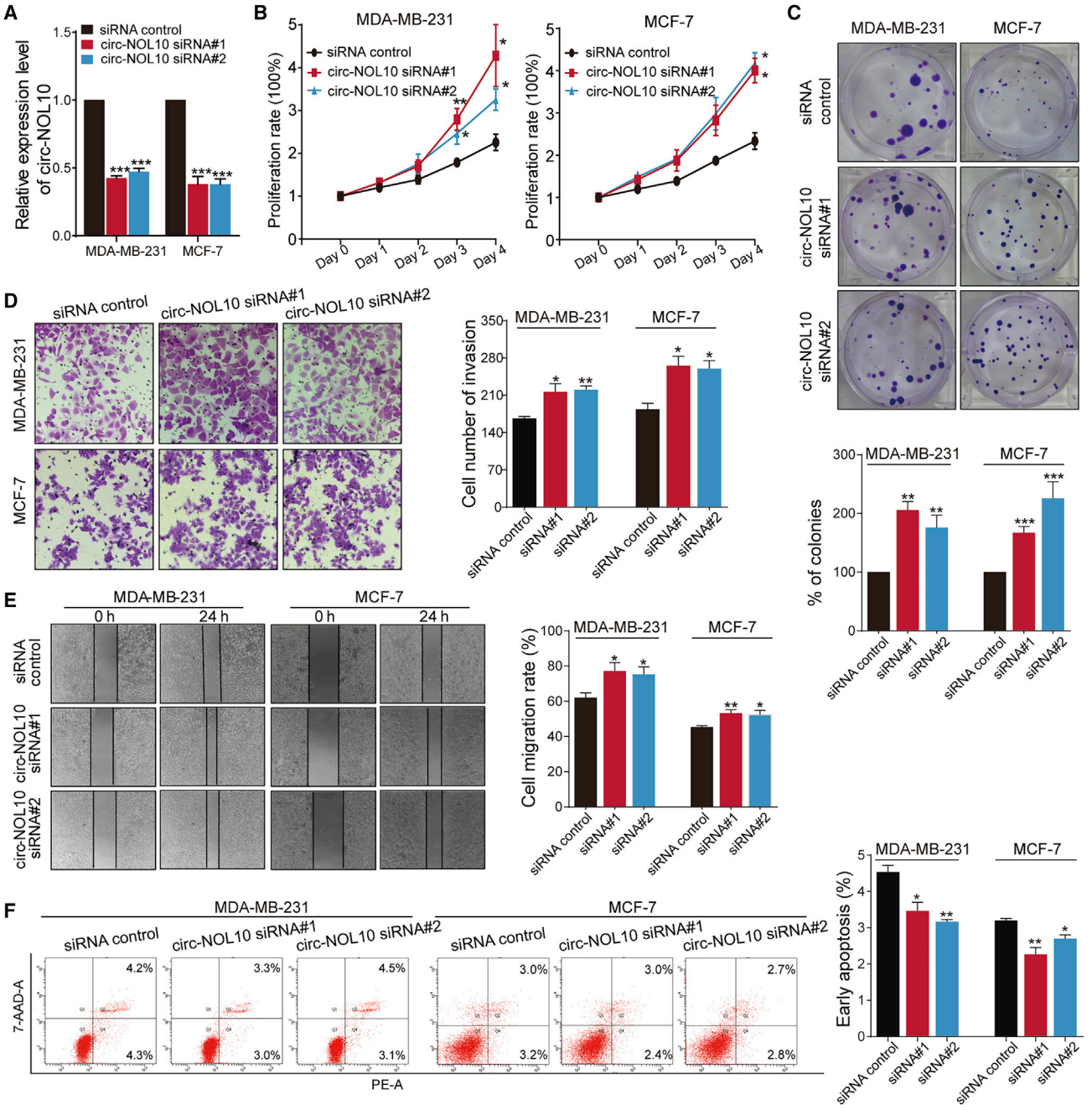


**Figure 3. Knockdown of circ-NOL10 promotes breast cancer progression**

Experiments were conducted after transfecting MCF-7 and MDA-MB-231 cells with circ-NOL10 siRNAs for 24 h. (A) circ-NOL10 expression after transfecting was analyzed by qPCR. (B) The effect of circ-NOL10 siRNAs on cell viability was analyzed by CCK-8. (C) The effect of circ-NOL10 siRNAs on colony formation was determined via a clonogenicity assay (top, representative pictures; bottom, quantitative bar for colony numbers). (D) The effect of circ-NOL10 siRNAs on cell invasion was detected via a Transwell assay (left, morphological comparison of cell penetration; right, quantitative bar for number of penetrating cells). (E) The effect of circ-NOL10 siRNAs on cell migration was measured by a wound scratch assay (left, representative images; right, quantitative bar for cell migration rate). (F) The effect of circ-NOL10 siRNAs on early apoptosis was analyzed by flow cytometry in cells (left, representative images; right, quantitative bar for cell apoptosis rate). Error bars represent the mean ± SEM from three independent experiments. *$p < 0.05$, **$p < 0.01$, ***$p < 0.001$.

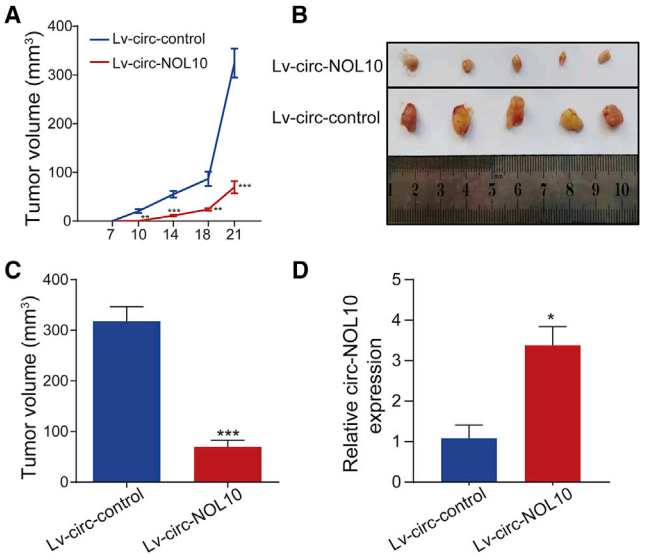


**Figure 4. Circ-NOL10 reduces tumor growth *in vivo***

(A) The tumor volumes in subcutaneous tumor-bearing nude mice at 7, 10, 14, 18, and 21 days. (B and C) Subcutaneous tumors were removed from nude mice at 21 days, and tumor weights were measured. (D) circ-NOL10 expression in tumors after removal from nude mice. *p < 0.05, **p < 0.01, ***p < 0.001.

promoted following transfection of miRNA inhibitors (Figure S2D). Accordingly, protein expression of *PDCD4* was upregulated significantly. Apoptosis-related markers, cleaved caspase-3 and *Bad*, were also increased significantly after downregulation of *miR-149-5p*, *miR330-3p*, and *miR452-5p* (Figures S2E and S2F). Upregulation of *circ-NOL10* induced PDCD4 and apoptosis marker expression, and the effects could be reversed by miR-149-5p, miR-330-3p, and miR-452-5p mimics (Figures S2G and S2H). These data indicate that *circ-NOL10* exerts a biological function via a *circ-NOL10/miR-149-5p/miR-330-3p/miR-452-5p/PDCD4* pathway.

### *MTDH* and *CASC3* regulate formation of *circ-NOL10* in breast cancer

An essential next step for understanding circRNA function is to identify key determinants in circRNA biogenesis. We reasoned that if a gene is a *bona fide* regulator, then it should have following characteristics: (1) alterations such as point mutation, copy number variation, and aberrant mRNA expression of this gene have been found in breast cancer, and (2) these alterations may have led to pathogenic changes and are correlated with survival. Based on these ideas, we analyzed multi-omics data of 825 BC samples and predicted 25 potential regulatory RBPs (materials and methods; Table S3). *ADAR* and *FUS* are involved in some circRNAs' life cycle.[22,23] Thus, combining our bioinformatics analysis and previous reports, we selected seven RBPs (*ADAR*, *FUS*, *SRSF1*, *CWC15*, *CASC3*, *MTDH*, and *ESRP1*) for further experiments. We constructed seven RBPs overexpression plasmids to examine whether they controlled aberrant expression of breast cancer-associated *circ-NOL10*. First, qPCR analyses showed that expression of *circ-NOL10* was downregulated in cells' ectopic expression of *CASC3* or *MTDH*, but cells treated with the other five RBPs did not show a consistent pattern (Figure S3A). OS analyses found that individuals with more alterations on these two RBPs had a poor prognosis in the BRCA dataset, suggesting that they play crucial roles in carcinogenesis (Figure S3B). A siRNA assay was used to further verify the association of *MTDH* and *CASC3* with *circ-NOL10* (Figures 7A and 7B). The qPCR results indicated that inhibition of *MTDH* and *CASC3* resulted in a significant increase of *circ-NOL10* in MDA-MB-231 and MCF-7 cells (Figure 7C). These findings confirmed that *CASC3* and *MTDH* could disrupt *circ-NOL10* expression.

An RNA immunoprecipitation (RIP) assay was performed to determine whether *MTDH* and *CASC3* can bind directly to *circ-NOL10*. Immunofluorescence and FISH (IF-FISH) analysis confirmed co-localization of *circ-NOL10* with *MTDH* and *CASC3* in the cytoplasm of MDA-MB-231 (Figure 7D). We transfected the pEZ-93-MTDH and pEZ-93-CASC3 plasmids, which express the encoded proteins fused to a FLAG tag, and individually overexpressed the two RBPs in MDA-MB-231 cells (Figure 7E). Bound complexes were pulled down using an antibody against FLAG. The qPCR results indicated that *circ-NOL10* was highly enriched in the FLAG-containing group compared with the immunoglobulin G (IgG) isotype control (Figure 7F). We further verified the interactions between *circ-NOL10* and endogenous RBPs by using a specific antibody against *CASC3* and *MTDH* (Figure 7G).

To determine the binding motifs, the immunoprecipitated RNAs were also sequenced on an Illumina NovaSeq 6000 system. Bioinformatics analyses of RIP-seq reads showed two putative binding sites of *MTDH* and one of *CASC3* on the *circ-NOL10* (Figure 7H). As shown in Figure 7I, the luciferase activity of the reporter with the wild-type *circ-NOL10* sequence (Luc-circ-NOL10) was inhibited significantly by *MDTH* and *CASC3*. This decrease was attenuated by mutation of *MDTH* binding sites (Luc-circ-N-mut A and Luc-circ-N-mut B) or the *CASC3* binding site (Luc-circ-N-mut C). These experimental results suggest that *CASC3* and *MTDH* bind *circ-NOL10* to regulate its formation in breast cancer. Importantly, these results also demonstrate that our bioinformatics predictions can be verified experimentally.

## DISCUSSION

Our results demonstrated that *circ-NOL10* inhibits breast cancer cell progression. Mechanistic studies indicated that *MTDH* and *CASC3* converge at downregulating *circ-NOL10* to release a set of three miRNAs. Competitive binding with the three miRNAs, in turn, blocks expression of the target gene *PDCD4*. Then decreased *PDCD4* inhibits apoptosis and promotes cell proliferation, migration, and invasion (Figure 8). Thus, *circ-NOL10* plays a central role in linking the upstream stimuli with downstream effectors in the RBP-ncRNA regulation network.

Accumulated evidence has shown correlations between circRNA expression and clinicopathological parameters such as tumor size, OS time, and tumor staging in various cancers.[13,24,25] Notably, our

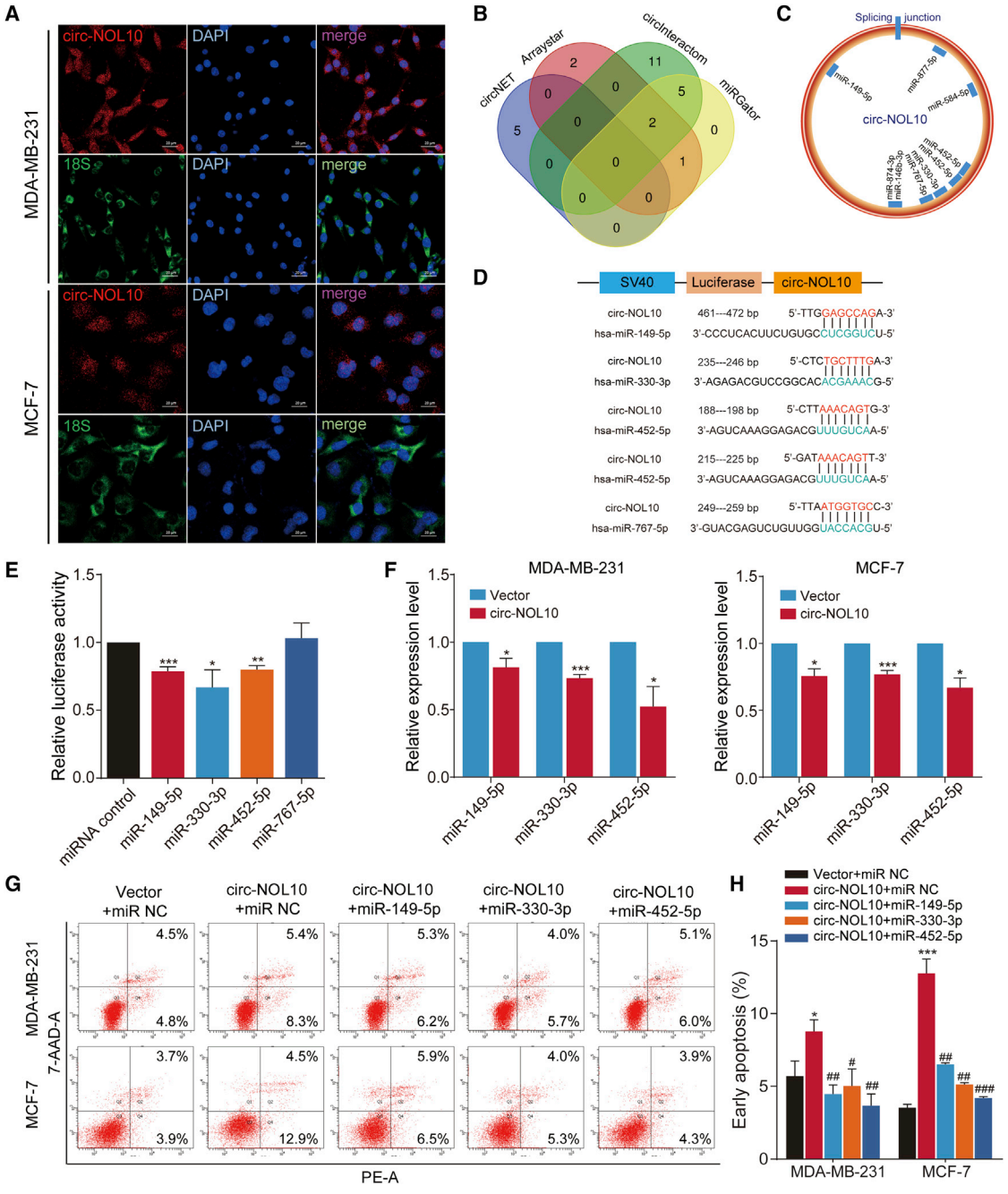


**Figure 5. Circ-NOL10 interacts with and sequesters miR-149-5p, miR-330-3p, and miR-452-5p in breast cancer cells**

(A) The distribution of circ-NOL10 in MDA-MB-231 and MCF-7 cells detected by FISH. Red, Cy3-labeled probes specific to circ-NOL10; green, FITC-labeled probes specific to 18S RNA; blue, DAPI stain for nuclei; merge represents an overlay figure. Scale bar, 20 μm. (B) Multiple bioinformatics tools were used to find miRNA and circ-NOL10 interaction. (C) An illustration showing the putative binding sites of circ-NOL10 with miRNAs. miR-452-5p has two binding sites. (D) A schematic of the psiCHECK2-circ-NOL10 vector and circ-NOL10 recognition sites. (E) Luciferase activity of psiCHECK2-circ-NOL10 co-transfected with selected miRNA mimics or control mimics was determined by a reporter assay. The relative luciferase activity was normalized with *Renilla* activity. (F) miRNA expression after transfection of the circ-NOL10 overexpression plasmid or a control vector in MDA-MB-231 cells (left panel) and in MCF-7 cells (right panel). (G and H) The effect of circ-NOL10 on early apoptosis after transfection of circ-NOL10 or co-transfection with miR-149-5p, miR-330-3p, or miR-452-5p in MDA-MB-231 and MCF-7 cells (left, representative images; quantitative bar for cell apoptosis rate). *, circ-NOL10+miR NC compared with vector+miR NC; #, circ-NOL10+miRNA compared with circ-NOL10+miR NC. *, #p < 0.05; **, ##p < 0.01; ***, ###p < 0.001.

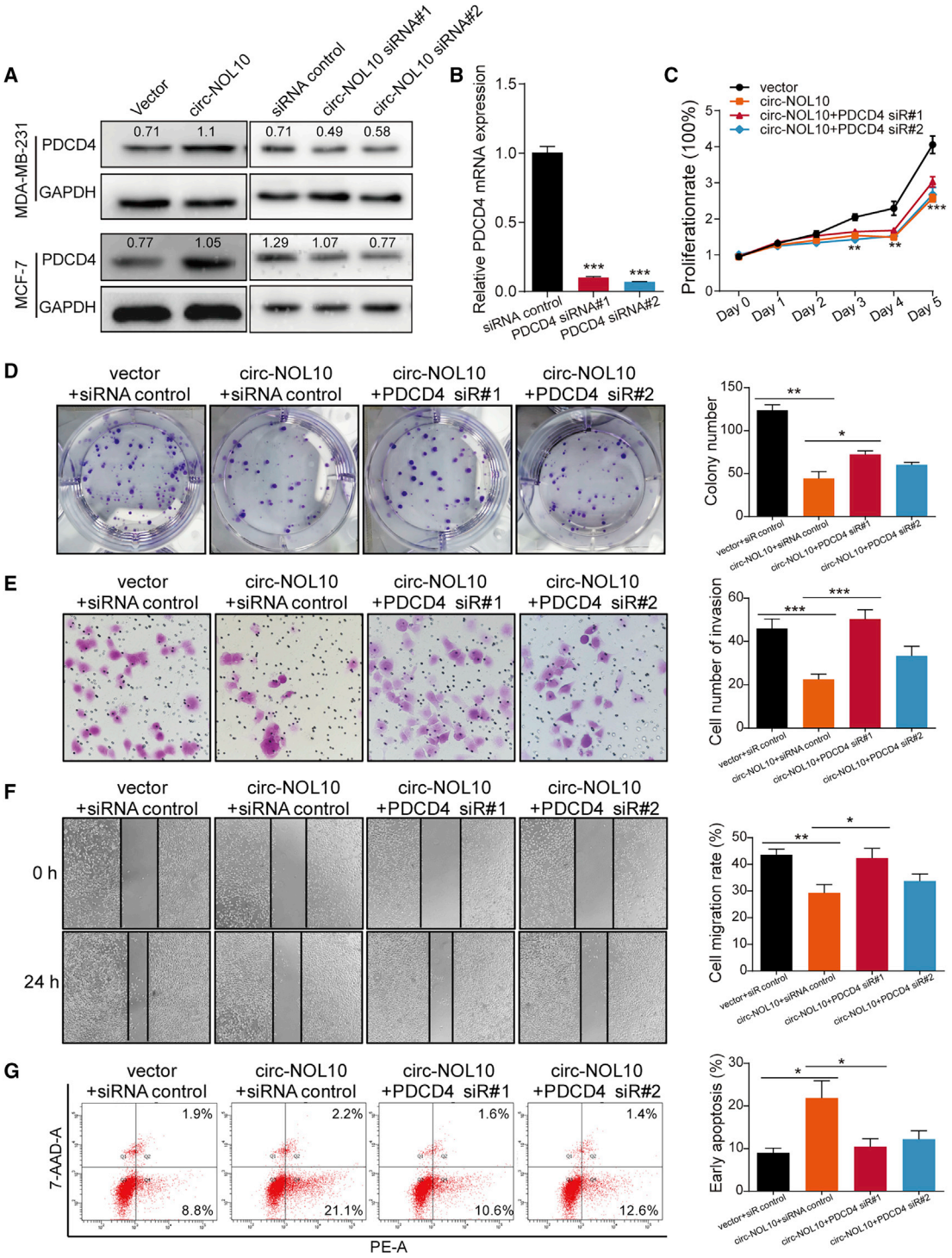


**Figure 6. Circ-NOL10 suppresses breast cancer progression by regulating PDCD4**

(A) Western blot of PDCD4 after transfection of the overexpression circ-NOL10 plasmid or siRNAs in cells. (B) Expression of PDCD4 mRNA was examined after transfection two different siRNAs in cells. (C) Cell viability was analyzed by CCK-8. (D) Colony formation was determined via a clonogenicity assay (left, representative pictures; right, quantitative bar for colony numbers). (E) Cell invasion was detected via a Transwell assay (left, morphological comparison of cell penetration; right, quantitative bar for number of penetrating cells). (F) Cell migration was measured by a wound scratch assay (left, representative images; right, quantitative bar for cell migration rate). (G) Early cell apoptosis was analyzed by flow cytometry in cells (left, representative images; right, quantitative bar for cell apoptosis rate). Error bars represent the mean ± SEM from three independent experiments. *p < 0.05, **p < 0.01, ***p < 0.001.

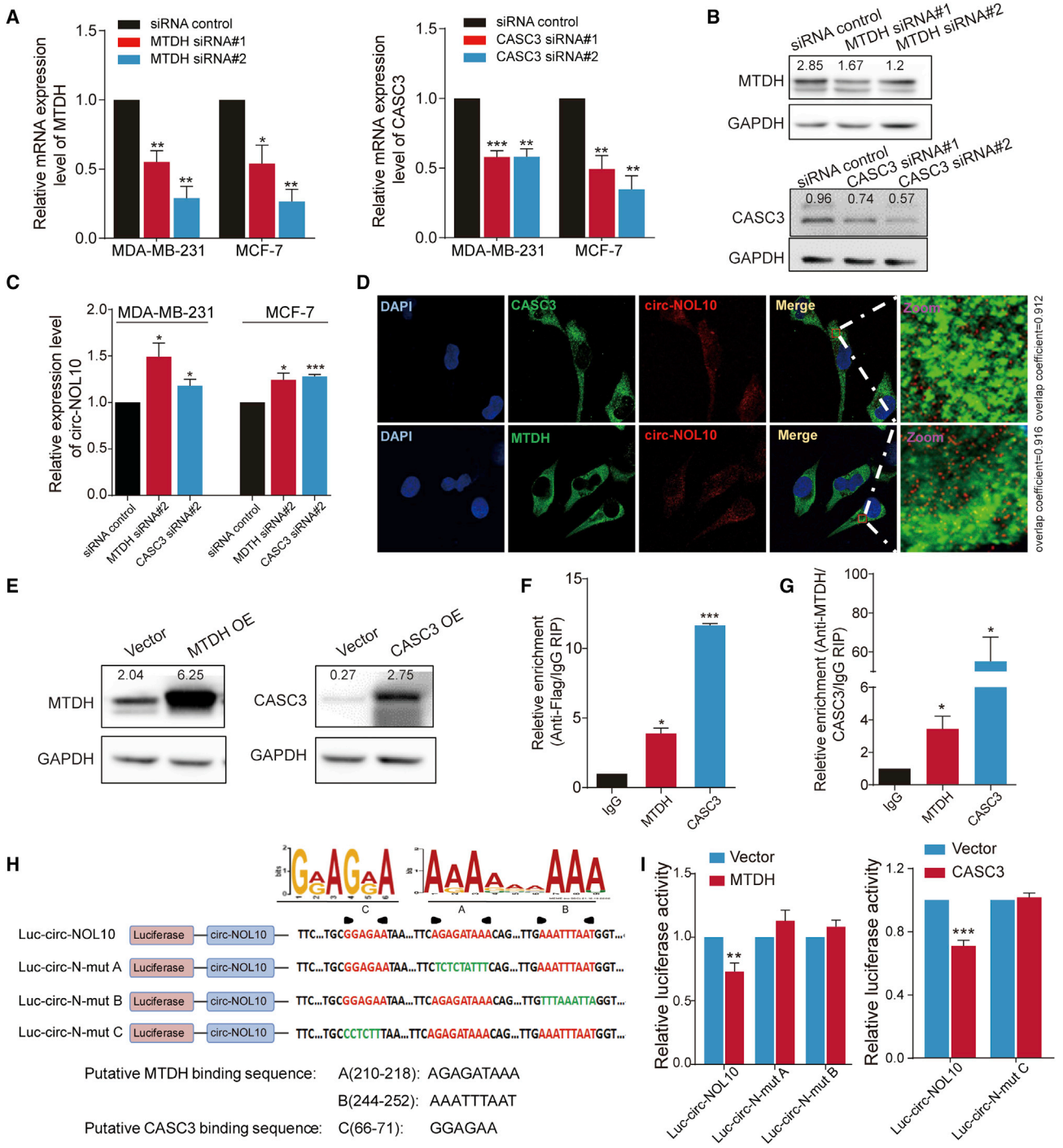


**Figure 7. MTDH and CASC3 regulate formation of circ-NOL10**

(A–C) After transfecting cells for 48 h with MTDH and CASC3 siRNA#1 and siRNA#2, (A) MTDH and CASC3 mRNAs were analyzed by qRT-qPCR, (B) MTDH and CASC3 proteins were analyzed by western blot, and (C) circ-NOL10 expression was analyzed by qPCR. (D) IF-FISH assay showing that circ-NOL10 colocalized with MTDH and CASC3 proteins in MDA-MB-231 cell cytoplasm. Red, Cy3-labeled probes specific to circ-NOL10; green, MTDH and CASC3 protein; blue, DAPI stain for nuclei; merge represents an overlay figure. (E) MTDH and CASC3 proteins were analyzed by western blot after overexpression of MTDH and CASC3 in MDA-MB-231 cells. (F) qPCR was used to measure circ-NOL10 binding to MTDH and CASC3 by using an antibody against FLAG pulled-down bound complexes. Values were normalized to the level of background RIP, as detected by an IgG isotype control. (G) qPCR was used to measure circ-NOL10 binding to endogenous MTDH and CASC3 by using specificity antibody

*(legend continued on next page)*

study found that expression of *circ-NOL10* is significantly lower in breast cancer, especially in the LA and TNBC subtypes. Based on a large cohort of individuals with TNBC, we have shown that *circ-NOL10* expression is correlated with clinical stage, lymphatic metastasis, recurrence, and survival. Downregulated *circ-NOL10* is also associated with poor prognosis. Thus, *circ-NOL10* can potentially be utilized as a promising diagnostic and prognostic biomarker for breast cancer.

Recently, a few RNA-binding proteins have been shown to control circRNA generation. For example, the splicing factor *ESRP1* can interact with the flanking regions of circ-BIRC6-forming exons to promote formation of *circ-BIRC6* in human embryonic stem cells.[26] Another report found that *ADAR1* mediates adenosine-to-inosine (A-to-I) RNA editing to inhibit circRNA production.[22,27] However, the proteins that drive the circRNA differential expression in breast cancer remain elusive. We found that *circ-NOL10* is highly inhibited in all subtypes of breast cancer compared with normal tissue. Previous reports have also indicated that *circ-NOL10* is expressed at low levels in breast, lung, and colorectal cancer.[28–30] This agreement suggests that *circ-NOL10* is a common player in carcinogenesis. Investigation in lung cancer also found that *circ-NOL10* is regulated by the splicing factor *ESRP1*. Although *ESRP1* is indeed a candidate, based on our bioinformatics analysis of its expression profile and genomic variations, the experimental results did not support its role in regulation (Figure S3A). This reflected the flexible mechanistic option when cells facing different circumstance. Instead, our integrative approach identified two RBPs, *MTDH* and *CASC3*, that regulate *circ-NOL10* expression in breast cancer.

*MTDH* was first identified as a mediator responsible for breast-to-lung cancer metastasis.[31] Compared with non-malignant tissues, it is expressed highly in many cancers, including breast, prostate, and liver cancer.[32–34] Subsequently, *MTDH* has been demonstrated to coordinate multiple signaling pathways implicated in various aspects of carcinogenesis and become an attractive novel therapeutic target.[35–38] Limited biological function is known for *CASC3* (also known as metastatic lymph node 51). It was first identified as core component of the exon junction complex.[39] Previous studies have established that it resides in the chromosome 17q12–q21 region, where amplifications occur frequently.[40] *CASC3* overexpression has been found in breast cancer and fibroblast-like synoviocytes from individuals with rheumatoid arthritis.[41,42] However, the role of *CASC3* in breast cancer progression remains unclear. We found that these two RBPs bind and repress *circ-NOL10*, which is expressed at low levels in breast cancer. Thus, this investigation not only adds a novel ncRNA link to the many signaling pathways involving *MTDH* but also opens a new chapter for elucidating *CASC3*'s functional consequences.

This investigation of the regulation of *circ-NOL10* and its biological functions and clinical implications in breast cancer should shed light on the circRNA-mediated mechanism in tumorigenesis.

## MATERIALS AND METHODS

### Clinical samples

16 normal mammary gland tissues and 178 breast cancer tissues were used in this study, which have been described previously in detail.[13]

### Cell culture

MCF-7, MDA-MB-231, T47D, BT20, BT549, SKBR3, MDA-MB-157, MDA-MB-435, MDA-MB-436, MDA-MB-468, MCF-10A, and 293T cells were purchased from the ATCC and cultured under conditions recommended by the ATCC.

### Oligos, plasmids, and transfection

siRNA oligonucleotides were designed and synthesized by GenePharma (Suzhou, China). miRNA mimics or inhibitors were designed and synthesized by IGEbio (Guangzhou, China) (sequences are listed in Table S4). To efficiently circularize a circRNA transcript in cells, the circ-NOL10-overexpressing plasmid was synthesized by Genechem (Shanghai, China). The overexpression plasmids pEZ-93-MTDH-FLAG, pEZ-93-CASC3-FLAG, pEZ-93-SRSF1-FLAG, pEZ-93- ESRP1-FLAG, pEZ-93-CWC15-FLAG, pEZ-M14-ADAR, and pEZ-M14-FUS were purchased from GeneCopoeia (Guangzhou, China). Cells were seeded in 6-well plates and cultured to 60%–70% confluence before transfection. Plasmids were transiently transfected using Lipofectamine 3000 (catalog number L3000015, Invitrogen, USA), and siRNA miRNA mimics, inhibitors, or corresponding controls were transiently transfected using Lipofectamine RNAiMAX (catalog number 13778150, Thermo Fisher Scientific, USA).

### RNA extraction and qPCR

Total RNA was extracted using Trizol reagent (Life Technologies, Carlsbad, CA, USA). For circRNA and mRNA analyses, cDNA was synthesized using the PrimeScript RT reagent kit (Takara, Japan). Quantitative PCR was performed using SYBR Premix Ex TaqII (Takara, Japan), and the reactions were subsequently measured on an ABI7500 PCR instrument (Thermo Fisher Scientific, Waltham, MA, USA). GAPDH was applied as an internal standard control. For miRNA analyses, cDNA synthesis was performed with miRNA-specific stem-loop primers using a Quantscript RT Kit (Ibsbio, Guangzhou, China). SYBR Premix Ex TaqII (Takara, Japan) was used for transcript quantification with specific primers on a LightCycler 96 PCR instrument (Roche, Basel, Switzerland). Primers were designed according to our previous study and are listed in Table S4.[13]

against CASC3 and MTDH. Values were normalized to the IgG isotype control. (H) Schematic illustrating luciferase reporters containing the circ-NOL10 sequence (Luc-circ-NOL10), mutated MTDH binding sites (Luc-circ-N-mut A and Luc-circ-N-mut B), and mutated CASC3 binding site (Luc-circ-N-mut C). The putative binding sites are colored in red, and the mutated sites (replaced by complementary sequences) are shown in green. (I) Reporter analyses showing the luciferase activity of Luc-circ-NOL10, Luc-circ-N-mut A, Luc-circ-N-mut B, and Luc-circ-N-mut C in 293 T cells ectopically expressing MTDH (left panel) or CASC3 (right panel). Quantitative data from three independent experiments are presented as mean ± SEM (error bars). *$p < 0.05$, **$p < 0.01$, ***$p < 0.001$.

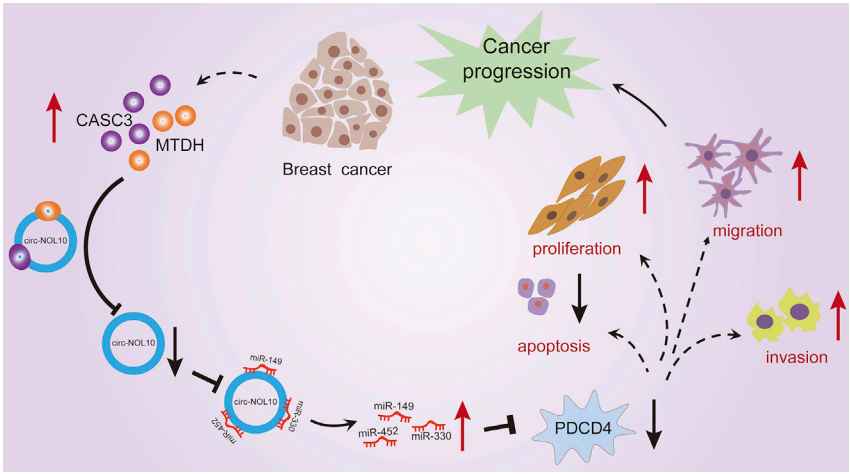


**Figure 8. Model of the RBP-ncRNA regulating network in breast cancer**

Altered MTDH and CASC3 bind and repress circ-NOL10, which further releases a set of three miRNAs. miRNAs bind to the target gene PDCD4 to inhibit its expression, promoting proliferation, migration, and invasion and decreasing apoptosis in breast cancer cells.

### Protein isolation and western blot analyses

Cells were lysed using RIPA lysis buffer (Biotechnology, China) containing a protease inhibitor cocktail (Roche, Switzerland). Proteins were separated by 10% SDS-PAGE, transferred to a polyvinylidene fluoride (PVDF) membrane (Millipore, MA, USA), incubated with 5% non-fat milk powder in TBST for 1 h at room temperature, and treated with specific primary antibodies overnight at 4°C. Then the membrane was incubated with a horseradish peroxidase (HRP)-conjugated secondary antibody, and each band was detected using an enhanced chemiluminescence kit (Millipore, MA, USA) and visualized with an enhanced chemiluminescence (ECL) BioImaging system (Azure, USA). Anti-CCBE1 was purchased from Biorbyt (catalog number orb215381). Anti-GAPDH, anti-caspase-3, and anti-cleaved caspase-3 antibodies were purchased from Cell Signaling Technology (catalog numbers 2118S, 9663S, and 9661S, respectively). TUSC2 antibodies were purchased from Affinity Bioscience (catalog number AF0500). Anti-glutamate receptor 3/GRIA3[EP813Y] and anti-Bad were purchased from Abcam (catalog numbers ab40845 and ab40845, respectively). Anti-PDCD4 antibodies were purchased from Santa Cruz Biotechnology (catalog number sc-376430).

### RNA FISH

FISH was performed as described previously in detail.[13] Cy3-labeled probes specific to *circ-NOL10* and fluorescein isothiocyanate (FITC)-labeled probes specific to 18S (Geneseed, Guangzhou, China; Table S4) were used in the hybridization. Nuclei were counterstained with 4,6-diamidino-2-phenylindole. The images were acquired on an Olympus FV3000 confocal microscope.

### RIP assays

The RIP assays were performed using the Magna RIP RNA-Binding Protein Immuno-Precipitation Kit (Millipore, MA, USA). In brief, MDA-MB-231 cells were harvested when they reached 90%. $2 \times 10^7$ cells were washed in ice-cold PBS and resuspended in 100 μL of RIP lysis buffer combined with a protease inhibitor cocktail and RNase inhibitors. 100 μL cell lysate was incubated with beads coated with 5 μg of control mouse IgG or an antibody against CASC3 (Santa Cruz, Dallas, TX, USA) and an antibody against MTDH (Abcam, Cambridge, MA, USA) or against FLAG with rotation at 4°C overnight. After the lysates were treated with proteinase K buffer, immunoprecipitated RNA was extracted and reverse transcribed using the PrimeScript RT reagent kit (Takara, Japan). The abundance of circ-NOL10 was detected by qPCR. The immunoprecipitated RNAs were also sequenced on an Illumina NovaSeq 6000 system using the KAPA Stranded RNA-Seq Library Prep Kit (Illumina, USA). Motif analyses was conducted by TREME with default settings.[43]

### Dual-luciferase reporter gene assay

The recombinant reporter plasmid (psiCHECK2_ Firefly_Luciferase-*Renilla*_Luciferase containing the circ-NOL10 sequence psiCHECK2-NOL10), reporters containing circ-NOL10-luc with mutated MTDH binding sites (Luc-circ-N-mut A and Luc-circ-N-mut B), and circ-NOL10-luc with a mutated CASC3 binding site (Luc-circ-N-mut C) were designed by IGEbio (Guangzhou, China). For the miRNA-circRNA interaction assay, HEK293T cells were co-transfected with the reporter plasmid and miR-149-5p, miR-330-3p, miR-452-5p mimic, or a negative control mimic and incubated for 24 h. For the RBP-circRNA interaction assay, cells were co-transfected with the reporter plasmid and MTDH or CASC3 overexpression plasmids and incubated for 48 h. Then luciferase activity was detected with a dual-luciferase reporter assay kit (Beyotime Biotechnology, China).

### IF-FISH co-localization assay

MDA-MB-231 cells were vaccinated in a confocal glass dish and fixed with 4% paraformaldehyde in PBS for 5 min. After washing three times with permeabilized with 0.1% Triton X-100 in PBS for 15 min, cells were added anhydrous ethanol 1 min and dried in the air. Cells were added with a denatured hybridization probe (Cy3-labeled probes specific to circ-NOL10, denatured at 88°C for 5 min, equilibrated at 4°C for 3 min) and incubated overnight at 37°C in a hybridization chamber. The next day, cells were rinsed with 2 × saline sodium citrate (SSC) preheated at 42°C for 5 min, and then rinsed with 2 × SSC at room temperature for 5 min twice. Then cells were blocked with 2% goat serum for 10 min at room temperature and incubated with primary antibody (MTDH antibody, Abcam, Cambridge, MA, USA and CASC3 antibody, Santa Cruz, Dallas, TX, USA) overnight at 4°C. On the third day, cells were washed with

PBS and then incubated with the corresponding Alexa 488-labeled secondary antibody for 1 h at room temperature, followed by staining the nucleus with DAPI. Fluorescence images were acquired using an Olympus FV3000 confocal microscope. The colocalization overlap coefficient was analyzed using Olympus FV3000 software.

### Cellular assays

#### *Wound healing assay*

MDA-MB-231 cells and MCF-7 cell were cultured in 6-well plates and transfected with a circ-NOL10-overexpressing plasmid or a control vector. The injury line was made with a 200-μL pipette tip when a monolayer of cells was plated in culture dishes at 100% confluence. Images of cell migration were captured at 0 and 24 h for MDA-MB-231 cells or at 48 h for MCF-7 cells. An average of eight random width of injury line was measured for quantization and normalized to the 0 h control and expressed as a relative migration rate. The assays were repeated at least three times.

#### *Colony formation assay*

Transfected MDA-MB-231 or MCF-7 cells were plated in 6-well plates at a density of 400 cells per well. Then cells were cultured for 14 days to form visible colonies. The cells were fixed with 4% paraformaldehyde and stained with 0.5% crystal violet, and then colonies were imaged and counted. The experiment was replicated at least three times.

#### *Cell proliferation assay*

Each well of $2 \times 10^3$ cells was seeded in five copies on a 96-well plate after MDA-MB-231 or MCF-7 cells were transfected for 48 h. 10 μL of CCK-8 reagent (Yeasen, China) was added to each well at 24, 48, 72, and 96 h and incubated at 37°C for 1 h. The optical density at 450 nm was measured using an automatic microplate reader (Synergy4, Bio-Tek, Winooski, VT, USA). The experiment was repeated three times.

#### *Matrigel invasion assay*

Transfected cells were serum starved for 24 h, and $2 \times 10^4$ MDA-MB-231 or MCF-7 cells in 200 μL serum-free medium were seeded in the upper chamber pre-coated with Matrigel (BD Biosciences, San Jose, CA, USA). 600 μL of complete medium was added to the lower chambers, and then the cells were incubated for 24 h. Cells were fixed with 4% paraformaldehyde and stained with 0.5% crystal violet. Invaded cells were counted in five random fields of view.

#### *Apoptosis assay*

Transfected cells were stained with PE/7-AAD (catalog number 557963, BD Biosciences, CA, USA) and incubated 15 min after trypsinization. Then treated cells were analyzed by a FACSCANTO II flow cytometer and FlowJo software (BD Biosciences, San Jose, CA, USA).

### Lentiviruses and tumor xenograft model

All animal experimental protocols were approved by the animal care and use Committee of Guangdong Medical UniversityA green fluorescent (ZsGreen) tagged circ-NOL10 OE vector (Lv-circ-NOL10) and blank vector (Lv-circ-control) were constructed and packaged in lentiviruses (HanBio, Shanghai, China). 4-week-old female nude mice were purchased from GemPharmatech (Nanjing, China) and kept under controlled conditions. Mice were divided randomly into 2 groups, with 5 mice in each group. Lv-circ-NOL10 and Lv-circ-control were transfected into MDA-MB-231 cells. Then MDA-MB-231 cells ($2 \times 10^6$ cells in 200 μL PBS solution) were inoculated subcutaneously into the left flanks of nude mice. The tumor volume was measured 1 week after injection and determined every 4 days, and the tumor volume ($V = L \times W2/2$, L represents the longest diameter, and W represents the shortest diameter) was recorded each time. The mice were killed, and tumor tissue was removed for further research after 21 days.

### Bioinformatics analysis

Potential miRNAs binding to circ-NOL10 are predicted by CircNet, CircInteractome, and Arraystar algorithms.[44,45] We selected miRNAs that are expressed abundantly in breast cancer samples based on the miRGator database.[46] To predict a potential regulator in cicRNA biogenesis, 1,344 RBP reported in previous literature were used for this analysis.[47] Multiple omics data were downloaded from the cBioPortal (http://www.cbioportal.org/), which includes somatic mutation, copy number variations, and differential mRNA expression in 825 breast-invasive carcinoma samples. The proportion of samples that harbors at least one of the above alterations was calculated. Furthermore, we ran a log rank test for each RBP to assess the association between gene alteration and survival time with R package "survival." RBPs that are altered in more than 10% of all cancer samples and correlated with survival ($p < 0.1$) are reported as potential circRNA regulators in breast cancer.

### Statistical analyses

Statistical analyses were performed using SPSS software with at least three independent experiments. The relationship between *circ-NO10* expression and clinical features was analyzed by independent t test. ROC curve analyses were performed using Prism 8.0 software (GraphPad, USA). DFS and OS curves were drawn using the Kaplan-Meier method. Univariate and multivariate Cox regression models were used to evaluate risk factors for breast cancer DFS and OS.

## SUPPLEMENTAL INFORMATION

Supplemental information can be found online at https://doi.org/10.1016/j.omtn.2021.09.013.

## ACKNOWLEDGMENTS

This work has been supported in part by the National Natural Science Foundation of China (81673037 and 91859120) and the Start-Up Fund for High Talents from Xiang'an Hospital of Xiamen University (PM201809170013). We thank Dr. Stanley Lin for editing this manuscript.

## AUTHOR CONTRIBUTIONS

J.X. and M.C. conceived the project and designed the experiments. Y.C., X.Z., Q.C., C.-C.S., Y.-X.O., J.F., and L.C. performed the

experiments. X.Z. and F.Z. contributed to acquisition and analysis of clinical data. J.X. and D.C. developed the computational pipeline. J.X. and M.C. collected and interpreted the data. J.X. wrote the manuscript. All authors read and approved the final manuscript.

## DECLARATION OF INTERESTS

The authors declare no competing interests.

## REFERENCES


1. Siegel, R.L., Miller, K.D., and Jemal, A. (2017). Cancer Statistics, 2017. CA Cancer J. Clin. *67*, 7–30.
2. Waks, A.G., and Winer, E.P. (2019). Breast Cancer Treatment: A Review. JAMA *321*, 288–300.
3. Wang, X., and Fang, L. (2018). Advances in circular RNAs and their roles in breast Cancer. J. Exp. Clin. Cancer Res. *37*, 206.
4. Zhao, X., Cai, Y., and Xu, J. (2019). Circular RNAs: Biogenesis, Mechanism, and Function in Human Cancers. Int. J. Mol. Sci. *20*, 3926.
5. Jeck, W.R., Sorrentino, J.A., Wang, K., Slevin, M.K., Burd, C.E., Liu, J., Marzluff, W.F., and Sharpless, N.E. (2013). Circular RNAs are abundant, conserved, and associated with ALU repeats. RNA *19*, 141–157.
6. Memczak, S., Jens, M., Elefsinioti, A., Torti, F., Krueger, J., Rybak, A., Maier, L., Mackowiak, S.D., Gregersen, L.H., Munschauer, M., et al. (2013). Circular RNAs are a large class of animal RNAs with regulatory potency. Nature *495*, 333–338.
7. Kristensen, L.S., Andersen, M.S., Stagsted, L.V.W., Ebbesen, K.K., Hansen, T.B., and Kjems, J. (2019). The biogenesis, biology and characterization of circular RNAs. Nat. Rev. Genet. *20*, 675–691.
8. Patop, I.L., Wüst, S., and Kadener, S. (2019). Past, present, and future of circRNAs. EMBO J. *38*, e100836.
9. Zhang, F., Zhao, X., Dong, H., and Xu, J. (2018). circRNA expression analysis in lung adenocarcinoma: comparison of paired fresh frozen and formalin-fixed paraffin-embedded specimens. Biochem. Biophys. Res. Commun. *500*, 738–743.
10. Bahn, J.H., Zhang, Q., Li, F., Chan, T.M., Lin, X., Kim, Y., Wong, D.T., and Xiao, X. (2015). The landscape of microRNA, Piwi-interacting RNA, and circular RNA in human saliva. Clin. Chem. *61*, 221–230.
11. Li, Y., Zheng, Q., Bao, C., Li, S., Guo, W., Zhao, J., Chen, D., Gu, J., He, X., and Huang, S. (2015). Circular RNA is enriched and stable in exosomes: a promising biomarker for cancer diagnosis. Cell Res. *25*, 981–984.
12. Zeng, K., He, B., Yang, B.B., Xu, T., Chen, X., Xu, M., Liu, X., Sun, H., Pan, Y., and Wang, S. (2018). The pro-metastasis effect of circANKS1B in breast cancer. Mol. Cancer *17*, 160.
13. Xu, J.Z., Shao, C.C., Wang, X.J., Zhao, X., Chen, J.Q., Ouyang, Y.X., Feng, J., Zhang, F., Huang, W.H., Ying, Q., et al. (2019). circTADA2As suppress breast cancer progression and metastasis via targeting miR-203a-3p/SOCS3 axis. Cell Death Dis. *10*, 175.
14. Chen, B., Wei, W., Huang, X., Xie, X., Kong, Y., Dai, D., Yang, L., Wang, J., Tang, H., and Xie, X. (2018). circEPSTI1 as a Prognostic Marker and Mediator of Triple-Negative Breast Cancer Progression. Theranostics *8*, 4003–4015.
15. Ren, S., Liu, J., Feng, Y., Li, Z., He, L., Li, L., Cao, X., Wang, Z., and Zhang, Y. (2019). Knockdown of circDENND4C inhibits glycolysis, migration and invasion by up-regulating miR-200b/c in breast cancer under hypoxia. J. Exp. Clin. Cancer Res. *38*, 388.
16. Wang, Q., Zhu, J., Wang, Y.W., Dai, Y., Wang, Y.L., Wang, C., Liu, J., Baker, A., Colburn, N.H., and Yang, H.S. (2017). Tumor suppressor Pdcd4 attenuates Sin1 translation to inhibit invasion in colon carcinoma. Oncogene *36*, 6225–6234.
17. Santhanam, A.N., Baker, A.R., Hegamyer, G., Kirschmann, D.A., and Colburn, N.H. (2010). Pdcd4 repression of lysyl oxidase inhibits hypoxia-induced breast cancer cell invasion. Oncogene *29*, 3921–3932.
18. Matsuhashi, S., Manirujjaman, M., Hamajima, H., and Ozaki, I. (2019). Control Mechanisms of the Tumor Suppressor PDCD4: Expression and Functions. Int. J. Mol. Sci. *20*, 2304.
19. Meric-Bernstam, F., Chen, H., Akcakanat, A., Do, K.A., Lluch, A., Hennessy, B.T., Hortobagyi, G.N., Mills, G.B., and Gonzalez-Angulo, A. (2012). Aberrations in translational regulation are associated with poor prognosis in hormone receptor-positive breast cancer. Breast Cancer Res. *14*, R138.
20. Chen, Z., Yuan, Y.C., Wang, Y., Liu, Z., Chan, H.J., and Chen, S. (2015). Down-regulation of programmed cell death 4 (PDCD4) is associated with aromatase inhibitor resistance and a poor prognosis in estrogen receptor-positive breast cancer. Breast Cancer Res. Treat. *152*, 29–39.
21. Meng, H., Wang, K., Chen, X., Guan, X., Hu, L., Xiong, G., Li, J., and Bai, Y. (2015). MicroRNA-330-3p functions as an oncogene in human esophageal cancer by targeting programmed cell death 4. Am. J. Cancer Res. *5*, 1062–1075.
22. Ivanov, A., Memczak, S., Wyler, E., Torti, F., Porath, H.T., Orejuela, M.R., Piechotta, M., Levanon, E.Y., Landthaler, M., Dieterich, C., and Rajewsky, N. (2015). Analysis of intron sequences reveals hallmarks of circular RNA biogenesis in animals. Cell Rep. *10*, 170–177.
23. Errichelli, L., Dini Modigliani, S., Laneve, P., Colantoni, A., Legnini, I., Capauto, D., Rosa, A., De Santis, R., Scarfò, R., Peruzzi, G., et al. (2017). FUS affects circular RNA expression in murine embryonic stem cell-derived motor neurons. Nat. Commun. *8*, 14741.
24. Chen, B., and Huang, S. (2018). Circular RNA: An emerging non-coding RNA as a regulator and biomarker in cancer. Cancer Lett. *418*, 41–50.
25. Kristensen, L.S., Hansen, T.B., Venø, M.T., and Kjems, J. (2018). Circular RNAs in cancer: opportunities and challenges in the field. Oncogene *37*, 555–565.
26. Yu, C.Y., Li, T.C., Wu, Y.Y., Yeh, C.H., Chiang, W., Chuang, C.Y., and Kuo, H.C. (2017). The circular RNA circBIRC6 participates in the molecular circuitry controlling human pluripotency. Nat. Commun. *8*, 1149.
27. Rybak-Wolf, A., Stottmeister, C., Glažar, P., Jens, M., Pino, N., Giusti, S., Hanan, M., Behm, M., Bartok, O., Ashwal-Fluss, R., et al. (2015). Circular RNAs in the Mammalian Brain Are Highly Abundant, Conserved, and Dynamically Expressed. Mol. Cell *58*, 870–885.
28. Nan, A., Chen, L., Zhang, N., Jia, Y., Li, X., Zhou, H., Ling, Y., Wang, Z., Yang, C., Liu, S., and Jiang, Y. (2018). Circular RNA circNOL10 Inhibits Lung Cancer Development by Promoting SCLM1-Mediated Transcriptional Regulation of the Humanin Polypeptide Family. Adv. Sci. (Weinh.) *6*, 1800654.
29. Wang, F., Wang, X., Li, J., Lv, P., Han, M., Li, L., Chen, Z., Dong, L., Wang, N., and Gu, Y. (2021). CircNOL10 suppresses breast cancer progression by sponging miR-767-5p to regulate SOCS2/JAK/STAT signaling. J. Biomed. Sci. *28*, 4.
30. Zhang, Y., Zhang, Z., Yi, Y., Wang, Y., and Fu, J. (2020). CircNOL10 Acts as a Sponge of miR-135a/b-5p in Suppressing Colorectal Cancer Progression via Regulating KLF9. OncoTargets Ther. *13*, 5165–5176.
31. Brown, D.M., and Ruoslahti, E. (2004). Metadherin, a cell surface protein in breast tumors that mediates lung metastasis. Cancer Cell *5*, 365–374.
32. Thirkettle, H.J., Girling, J., Warren, A.Y., Mills, I.G., Sahadevan, K., Leung, H., Hamdy, F., Whitaker, H.C., and Neal, D.E. (2009). LYRIC/AEG-1 is targeted to different subcellular compartments by ubiquitinylation and intrinsic nuclear localization signals. Clin. Cancer Res. *15*, 3003–3013.
33. Tokunaga, E., Nakashima, Y., Yamashita, N., Hisamatsu, Y., Okada, S., Akiyoshi, S., Aishima, S., Kitao, H., Morita, M., and Maehara, Y. (2014). Overexpression of metadherin/MTDH is associated with an aggressive phenotype and a poor prognosis in invasive breast cancer. Breast Cancer *21*, 341–349.
34. Robertson, C.L., Mendoza, R.G., Jariwala, N., Dozmorov, M., Mukhopadhyay, N.D., Subler, M.A., Windle, J.J., Lai, Z., Fisher, P.B., Ghosh, S., and Sarkar, D. (2018). Astrocyte Elevated Gene-1 Regulates Macrophage Activation in Hepatocellular Carcinogenesis. Cancer Res. *78*, 6436–6446.
35. Wan, L., Lu, X., Yuan, S., Wei, Y., Guo, F., Shen, M., Yuan, M., Chakrabarti, R., Hua, Y., Smith, H.A., et al. (2014). MTDH-SND1 interaction is crucial for expansion and activity of tumor-initiating cells in diverse oncogene- and carcinogen-induced mammary tumors. Cancer Cell *26*, 92–105.
36. Hu, G., Wei, Y., and Kang, Y. (2009). The multifaceted role of MTDH/AEG-1 in cancer progression. Clin. Cancer Res. *15*, 5615–5620.

37. Srivastava, J., Robertson, C.L., Rajasekaran, D., Gredler, R., Siddiq, A., Emdad, L., Mukhopadhyay, N.D., Ghosh, S., Hylemon, P.B., Gil, G., et al. (2014). AEG-1 regulates retinoid X receptor and inhibits retinoid signaling. Cancer Res. *74*, 4364–4377.

38. Liang, Y., Hu, J., Li, J., Liu, Y., Yu, J., Zhuang, X., Mu, L., Kong, X., Hong, D., Yang, Q., and Hu, G. (2015). Epigenetic Activation of TWIST1 by MTDH Promotes Cancer Stem-like Cell Traits in Breast Cancer. Cancer Res. *75*, 3672–3680.

39. Bono, F., Ebert, J., Lorentzen, E., and Conti, E. (2006). The crystal structure of the exon junction complex reveals how it maintains a stable grip on mRNA. Cell *126*, 713–725.

40. Arriola, E., Marchio, C., Tan, D.S., Drury, S.C., Lambros, M.B., Natrajan, R., Rodriguez-Pinilla, S.M., Mackay, A., Tamber, N., Fenwick, K., et al. (2008). Genomic analysis of the HER2/TOP2A amplicon in breast cancer and breast cancer cell lines. Lab. Invest. *88*, 491–503.

41. Degot, S., Régnier, C.H., Wendling, C., Chenard, M.P., Rio, M.C., and Tomasetto, C. (2002). Metastatic Lymph Node 51, a novel nucleo-cytoplasmic protein overexpressed in breast cancer. Oncogene *21*, 4422–4434.

42. Jang, J., Lim, D.S., Choi, Y.E., Jeong, Y., Yoo, S.A., Kim, W.U., and Bae, Y.S. (2006). MLN51 and GM-CSF involvement in the proliferation of fibroblast-like synoviocytes in the pathogenesis of rheumatoid arthritis. Arthritis Res. Ther. *8*, R170.

43. Bailey, T.L. (2011). DREME: motif discovery in transcription factor ChIP-seq data. Bioinformatics *27*, 1653–1659.

44. Dudekula, D.B., Panda, A.C., Grammatikakis, I., De, S., Abdelmohsen, K., and Gorospe, M. (2016). CircInteractome: A web tool for exploring circular RNAs and their interacting proteins and microRNAs. RNA Biol. *13*, 34–42.

45. Liu, Y.C., Li, J.R., Sun, C.H., Andrews, E., Chao, R.F., Lin, F.M., Weng, S.L., Hsu, S.D., Huang, C.C., Cheng, C., et al. (2016). CircNet: a database of circular RNAs derived from transcriptome sequencing data. Nucleic Acids Res. *44* (D1), D209–D215.

46. Cho, S., Jang, I., Jun, Y., Yoon, S., Ko, M., Kwon, Y., Choi, I., Chang, H., Ryu, D., Lee, B., et al. (2013). MiRGator v3.0: a microRNA portal for deep sequencing, expression profiling and mRNA targeting. Nucleic Acids Res. *41*, D252–D257.

47. Neelamraju, Y., Hashemikhabir, S., and Janga, S.C. (2015). The human RBPome: from genes and proteins to human disease. J. Proteomics *127* (Pt A), 61–70.